

Central-Symmetry Decoupling Technique for Circularly-Polarized MIMO System of Tightly Packed Chinese-character Shaped Patch Antennas

Kwok L. Chung¹, Aiqi Cui¹, Mingliang Ma¹, Botao Feng², and Yingsong Li^{3*}

¹ Civionics Research Laboratory, School of Civil Engineering
Qingdao University of Technology, Qingdao, 266033, China
klchung@qut.edu.cn

² College of Electronic and Information Engineering, Shenzhen University, 518060, China
fengbotao@szu.edu.cn

³ College of Information and Communication Engineering, Harbin Engineering University, Harbin, 15001, China
*liyingsong@ieee.org

Abstract — This article presents a novel decoupling technique for the circularly polarized multiple-input-multiple-output (CP-MIMO) system composed of *Guo*-shaped patch antennas. A comparative study has been conducted on antenna performance as a function of packing distance before and after applying the technique. A prototype of two-element *Guo*-shaped patch MIMO at a small inter-element spacing of 12.5 mm has devised aiming for the 5G new radio n38 (2.57-2.62 GHz) applications. Simulation reinforced with experimental results confirmed the effectiveness of the proposed technique, whereas the two *Guo*-shaped patch elements packed in such small spacing can be operated independently. Both the envelope correlation coefficient and diversity gain are approaching their ideal values.

Index Terms — Antenna isolation, artistic patch antenna, Chinese-character-shaped patch antenna, CP-MIMO, decoupling technique.

I. INTRODUCTION

Multiple-input-multiple-output (MIMO) antenna system becomes the key technology in current wireless communications addressing the demands of high channel capacity and anti-multipath interferences [1]. The circularly polarized (CP) antennas play a crucial role in space and indoor communications owing to the advantages of non-line-of-sight, better mobility and robust to polarization mismatching as compared with the linearly polarization (LP) counterparts [2-3]. As a result, the CP-MIMO antenna systems have been investigated and become popular in recent years. It has demonstrated that the achievable channel capacity of CP-MIMO outperforms the LP counterparts, especially when antennas are not perfectly aligned. Moreover, CP-MIMO allows yielding superior performance when its 3-dB

axial-ratio beamwidth coverage reaches $\sim 40^\circ$ [4].

Suppression techniques of mutual coupling between antennas have long been the research topics in antenna array systems [3, 5-9]. Decoupling or isolation necessity is the primary design goal in MIMO systems. In [3], angular offset elements were used to reduce the mutual coupling and gain enhancement, this type of method is classified as the self-decoupled method. Various types of defected ground structure (DGS) [5-7] were employed to enhance the isolation between elements, whereas a wheel-like metamaterial decoupling structure was presented in [8]. In [9-12], different insertion techniques were used to enhance the isolation of MIMO antennas. For the aim of mutual coupling reduction, radial stub loaded resonator [9] and 3-D metamaterial structure [10] were inserted respectively in between the two elements of MIMOs. Also, the multi-layer electromagnetic bandgap structure and the single-layer metamaterial superstrate were added into the two-element source antennas in [11] and [12], respectively. In the recent CP-MIMO designs, a simple microstrip line was used as the decoupling structure [13], whereas a hybrid technique of parasitic patch with diagonal position of dielectric resonator antennas was presented for WiMAX application [14]. For 5G millimeter-wave bands, a high-gain wideband CP antenna with MIMO capabilities based on Fabry-Perot resonant cavity was proposed in [15], wherein a single-layered dielectric slab of half-wavelength thickness was utilized as a partially reflecting surface so that a high isolation of higher than 20 dB was obtained for an interelement spacing of half-wavelength. A dual CP-MIMO antenna using a hybrid technique was also reported in [16], wherein three grounded stubs plus mirrored F-shaped DGS were included between microstrip-line fed near-square-patch antennas to achieve high isolation. However, the use of DGS creates

backward radiation leading to low forward directivity. The inclusions of additional resonators and or reflecting (metamaterial) surface may increase the antenna volume as well as the insertion loss.

In this article, a novel decoupling technique is proposed for the isolation enhancement of a closely packed *Guo*-shaped patch antenna array, wherein the two *Guo*-shaped patch elements are placed at a center-to-center (C2C) distance of 80 mm (0.69 free-space wavelengths at 2.6 GHz). The technique uses no additional resonator(s), no defected ground structure(s) and or metasurface/metamaterial. Instead, we altered one of the *L*-shaped feeds with its position and orientation central-symmetrically with respect to the original one. The results demonstrated that the proposed technique is able to enhance the isolation by 5 dB at a shortest C2C distance of 70 mm. Therefore, the axial ratio and broadside gain can be independently established without mutually deteriorated by strong mutual coupling. The 2.6-GHz CP-MIMO is devised for use at 5G NR n38.

II. CLOSELY PACKED TWO-ELEMENT *GUO*-SHAPED PATCH MIMO ANTENNAS

A. Geometry of CP *Guo*-shaped patch antenna

This section introduces the geometry of the Chinese character-shaped patch antenna, which is a modification of the *Guo*-shaped patch [17] for left-hand CP (LHCP) propagation. Figure 1 shows the top- and side-view geometry, where a *L*-shaped feeding probe is placed at a coordinate (m, n) with respect to the patch center and its arm is faced downward for LHCP generation. The geometrical parameters are summarized in Table 1.

Table 1: Geometrical parameters (unit: mm)

L	M	w	H	a
71.8	67.5	35.5	15.5	10.5
b	c	d	e	f
9.1	8.9	6.7	7.7	6.2
g	m	n	F_h	F_v
8.6	20.0	13.4	13.5	11.5

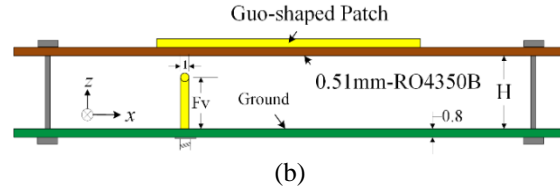
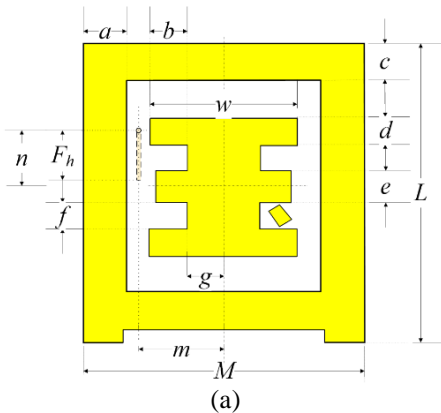


Fig. 1. Geometry of CP *Guo*-shaped element: (a) top view and (b) side view. The dielectric layer is 0.51mm thick RO4350B.

B. Impedance matching

Here, we present the effects of mutual coupling (MC), using Microwave Studio CST [18], when two identical *Guo*-shaped patch elements are closely packed at a C2C distance of D , namely, at an inter-element spacing of g , as shown in Fig. 2 (a). That is, when D is set at 70, 80, 90 and 100 mm, g is 2.5, 12.5, 22.5 and 32.5 mm, respectively. It is expected that the MC is very strong while the elements are placing closely, say 70 mm, as a result, the impedance matching in terms of reflection coefficients ($|S_{11}|$ and $|S_{22}|$) of both the elements deteriorated as shown in Figs. 2 (b) to 2 (e). At $D = 70$ mm, the very strong MC causes S_{11} and S_{22} in dB to increase and be unequal. The mutual coupling logically reduced with D increasing. At last, the effect becomes minimal when $D = 100$ mm so that the S_{11} and S_{22} curves have overlapped each other.

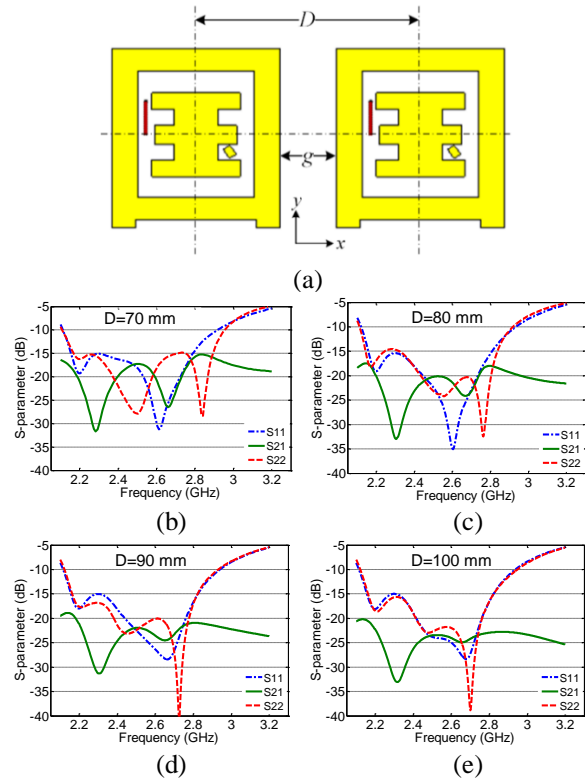


Fig. 2. Mutual coupling effect versus D .

C. Axial ratio and broadside gain performance

Strong MC not only affects the impedance matching but also the axial ratio (AR) and broadside gain (BG) performance of CP antennas. However, these were seldom fully addressed in the previous studies. Figure 3 demonstrates the comparison of AR and BG under two separation cases of 80 and 100 mm, respectively. At $D = 80$ mm, both the AR and BG curves deteriorated particularly, the deteriorations on the right-hand-side element (AR-R and BG-R) are more serious than the left-hand-side ones, which is attributed to the closer feed next to the left-element. Until the separation away at 100 mm, the situations are observed to be relieved. Therefore, a technique must be used to mitigate the mutual coupling effects at the closing space. An exploration of optimization issue arising during the modeling of *Guo*-shaped patch. The AR performance is very sensitive with the feed-probe location and orientation as compared with the BG and S-parameter performance. Therefore, a systematic tuning was used to obtain the best feed location by firstly aiming at AR performance.

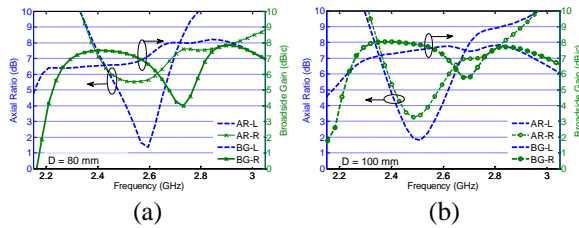


Fig. 3. Simulated performance of axial ratio and broadside gain for (a) $D = 80$ mm and (b) $D = 100$ mm.

II. CENTRAL-SYMMETRICAL TECHNIQUE APPLIED FOR TWO-ELEMENT ARRAY

It is known that most of single-feed CP patch antennas have more than one optimal feed location to achieve the same sense (handedness) of CP operation at the broadside direction [19]. In particular, when the patch antenna has a symmetrical geometry [20]. Here, we make use of this knowledge and move one of the feeding probes of closely packed elements in such a way that the two probes are central-symmetrical (CS) placed, as shown in Fig. 4. Note that the probe orientation of the horizontal arm is also placed CS.

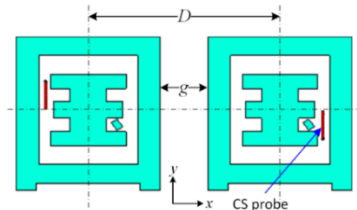


Fig. 4. Central-symmetrical technique is applied in the right-hand side element.

A. Effects on impedance matching

Figures 5 (a) to 5 (d) show the impedance matching in terms of S_{11} and S_{22} after applying the CS technique. As compared with Fig. 2, better reflection coefficients are obtained, particularly, in the closely packed case of $D = 70$ mm. One can see that the two elements are now almost isolated from each other. Besides, the mutual coupling reduced to below -20 dB for all separations.

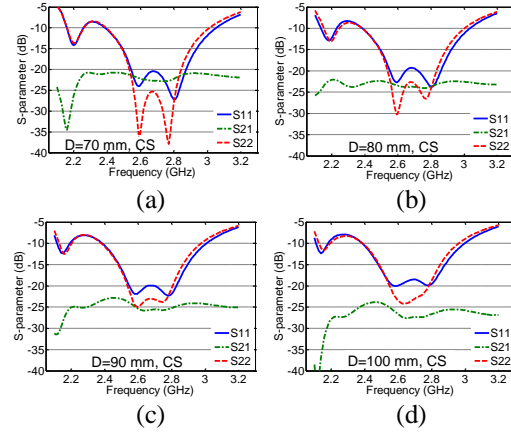


Fig. 5. Mutual coupling effects on reflection coefficients (S_{11} , S_{22}) as a function of separation D , after CS technique applied.

B. Isolation enhancement

The positive value of MC is the isolation between two input ports of the *Guo*-shaped patch element. We extracted that from Figs. 2 and 5, and make a comparison as a function of D , as shown in Figs. 6 (a) and 6 (b), respectively. Without using CS technique, the smaller the separation gives the more fluctuation on the isolation curves in the frequency range of 2-3 GHz. At the center frequency of 2.6 GHz, the isolation drops below 18 dB at 70 mm separation and enhanced to 23 dB at 100 mm. After applying CS, the isolation between *Guo*-shaped patch antennas is enhanced from 18 dB to a minimum of 22 dB at $D = 80$ mm across the whole frequency range. The simulated surface current distributions of the two closely packed *Guo*-shaped patch elements at 2.6 GHz shown in Fig. 7 are used to study the decoupling mechanism. In either case, the associated current with the *L*-probes are observed to be minimum.

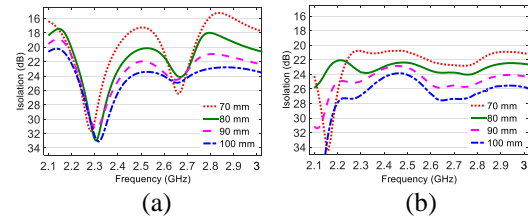


Fig. 6. Isolation comparison (a) before and (b) after applying central-symmetrical feeding for a number of separations.

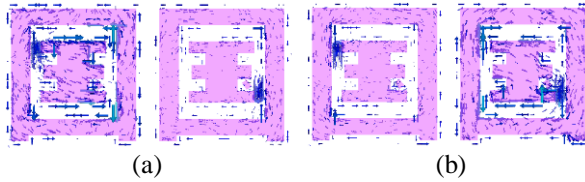


Fig. 7. Surface current plots when (a) left-element is excited, and (b) right-element is excited.

C. Axial ratio and broadside gain performance

After applying the central-symmetrical technique, Figs. 8 (a) and 8 (b) show the simulated AR and BG for the two cases, $D = 80$ and 100 mm, respectively. With reference to Figs. 4 (a) and 4 (b), both the AR and BG improved significantly. In particular, the performance of the right-hand-side element has almost the same as the left-hand-side element in both the cases. These validate the effectiveness of the CS technique in the far-field performance.

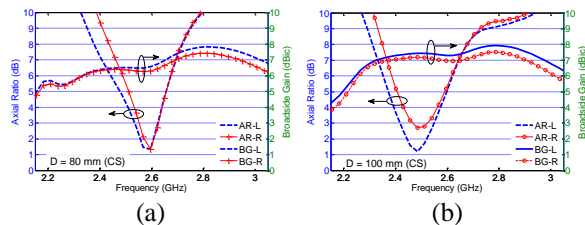


Fig. 8. Simulated *on-axis* axial ratio and broadside gain after applying CS technique: (a) $D = 80$ mm and (b) $D = 100$ mm.

III. FABRICATION AND EXPERIMENTAL VERIFICATION

A. S-parameter performance measurement

Prototypes of closely packed *Guo*-shaped patch antennas at $D = 80$ mm ($g = 12.5$ mm, $0.10\lambda_0$) with and without central-symmetry decoupling were fabricated and measured. A photograph of the prototype is depicted in Fig. 9, whereas their measured S-parameters are shown in Fig. 10. It can be seen that the measured mutual coupling (S_{21}) is suppressed to -25 dB at 2.6 GHz whereas the reflection coefficients of both antennas (S_{11} , S_{22}) are almost identical. This means that the *Guo*-shaped patch antennas now own sufficient isolation that can be operated without mutual affections. When further comparing with the simulated results shown in Fig. 5 (b), we can conclude that excepting the minor frequency shifts of S_{11} and S_{22} curves, the experimental results have validated the effectiveness of the CS technique.



Fig. 9. Photograph of CP MIMO with closely packed ($D = 80$ mm) *Guo*-shaped patch antennas.

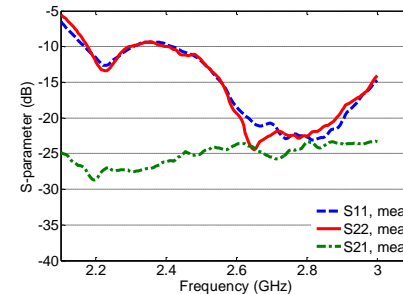


Fig. 10. Measured S-parameters of closely packed ($D = 80$ mm) *Guo*-shaped patch antennas after applying CS technique.

B. Measured axial ratio and broadside gain

The measurement of MIMO far-field performance was conducted inside a near-field SATIMO chamber, as depicted in Fig. 11. Besides, Fig. 12 displays the comparisons on AR and BG for both the left- and right-element. As verified before, the isolation is sufficiently high to cause the closely packed antennas to work independently. Both the ARs and BGs now also had very close performance. The measured 3-dB AR bandwidth is 2.56 - 2.64 GHz (3.1%), whereas the BG recorded as 6.5 dBc at 2.6 GHz. Moreover, the measured radiation patterns of both *Guo*-shaped elements at 2.6 GHz are plotted as shown in Fig. 13. As seen, the beam diversity can be achieved by using such novel probing technique.



Fig. 11. Far-field measurement undertaken inside SATIMO.

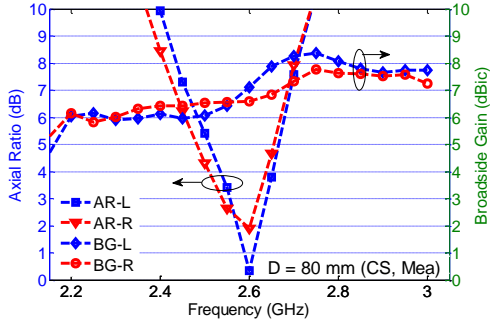


Fig. 12. Measured axial ratio and broadside gain after applying CS technique.

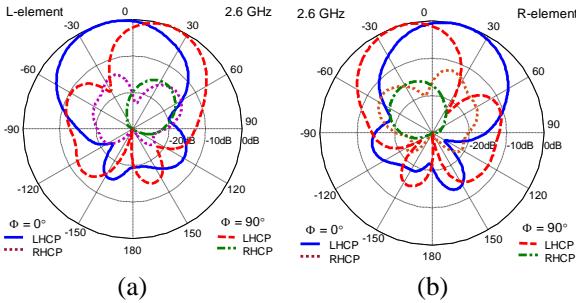


Fig. 13. Simulated and measured envelope correlation.

C. MIMO performance verifications

The envelope correlation coefficient (ECC) is known as a primary diversity performance metric of the MIMO antenna system. When all elements are excited, ECC indicates the level of mutual influences and the far-field correlation among antenna elements, which is expressed in terms of S-parameters as [21]:

$$ECC = \frac{|S_{11}^* S_{12} + S_{21}^* S_{22}|^2}{(1 - |S_{11}|^2 - |S_{21}|^2)(1 - |S_{21}|^2 - |S_{22}|^2)}, \quad (1)$$

the value of diversity-gain (DG) can then be obtained by using (2),

$$DG = 10\sqrt{1 - (ECC)^2}. \quad (2)$$

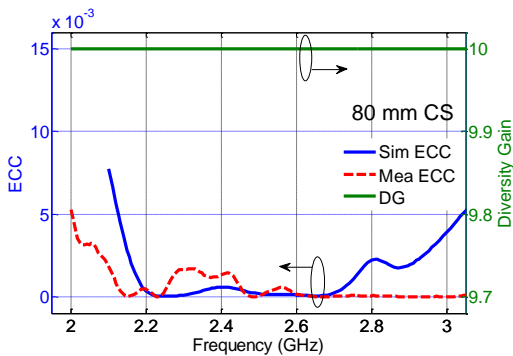


Fig. 14. Simulated and measured envelope correlation coefficients (ECCs) after applying CS technique.

Figure 14 shows the comparison of measured and simulated ECCs after using CS. As the ECCs are really small (0.002), the figure also shows that the diversity gains reach the upper limit of 10. Again, these values validate the effectiveness of the decoupling technique.

VI. CONCLUSION

A central-symmetrical technique is proposed for element decoupling in this paper. Two *Guo*-shaped patch elements, which were closely packed in a CP MIMO system at 2.6 GHz, were investigated. Simulated results, in terms of S-parameters, axial ratio and broadside gain have demonstrated that the proposed technique can effectively enhance the isolation so that the elements can be activated independently. Moreover, experimental results show that even at a small inter-element spacing of 12.5 mm ($0.108\lambda_0$ at 2.6 GHz), the measured ECC and DG approaching the ideal values of 0 and 10, respectively. Importantly, the technique uses no extra resonators or defected ground structures to achieve the results.

ACKNOWLEDGMENT

This work was supported by Funding of Key Laboratory of Advanced Marine Communication and Information Technology, MIIT, China (AMCIT2101-03) and the Fundamental Research Funds for the Central Universities (3072021CF0804) and the Open Project of State Key Laboratory of Millimeter Waves (K2020017).

REFERENCES

- [1] M. A. Jensen and J. W. Wallace, "A review of antennas and propagation for MIMO wireless communications," *IEEE Trans. Antennas Propag.*, vol. 52, no. 11, pp. 2810-2824, Nov. 2004.
- [2] K. L. Chung, X. Yan, Y. Li, and Y. Li, "A Jia-shaped artistic patch antenna for dual-band circular polarization," *Intern. J. Electronics and Comm. (AEÜ)*, vol. 120, 153207, June 2020.
- [3] K. L. Chung and S. Kharkovsky, "Mutual coupling reduction and gain enhancement using angular offset elements in circularly polarized patch array," *IEEE Antennas Wireless Propag. Lett.*, vol. 12, pp. 1122-1124, Sep. 2013.
- [4] F. A. Dicandia, S. Genovesi, and A. Monorchio, "Analysis of the performance enhancement of MIMO systems employing circular polarization," *IEEE Trans. Antennas Propag.*, vol. 65, no. 9, pp. 4824-4835, July 2017.
- [5] R. Anitha, V. P. Sarin, P. Mohanan, and K. Vasudevan, "Enhanced isolation with defected ground structure in MIMO antenna," *Electron. Lett.*, vol. 50, no. 24, pp. 1784-1786, 2014.
- [6] G. Zhang and Q. Chen, "Mutual coupling reduction in Chinese character-shaped artistic MIMO antenna," *Microw. Optical Tech. Lett.*, vol. 61, no. 7, pp. 2588-2594, July 2020.

- [7] C.-M. Luo, J.-S. Hong, and L.-L. Zhong, "Isolation enhancement of a very compact UWB-MIMO slot antenna with two defected ground structures," *IEEE Antennas Wireless Propag. Lett.*, vol. 14, pp. 1766-1769, 2015.
- [8] J. Jiang, Y. Xia, and Y. Li, "High isolated X-band MIMO array using novel wheel-like metamaterial decoupling structure," *Applied Computational Electromagnetics Society Journal*, vol. 34, no. 12, pp. 1829-1836, 2019.
- [9] Y. Li, W. Li, and W. Yu, "A multi-band/UWB MIMO/diversity antenna with an enhanced isolation using radial stub loaded resonator," *Applied Computational Electromagnetics Society Journal*, vol. 28, no. 1, pp. 8-20, 2013.
- [10] K. Yu, Y. Li, and X. Liu, "Mutual coupling reduction of a MIMO antenna array using 3-D novel metamaterial structures," *Applied Computational Electromagnetics Society Journal*, vol. 33, no. 7, pp. 758-763, 2018.
- [11] T. Jiang, T. Jiao, and Y. Li, "A low mutual coupling MIMO antenna using periodic multi-layered electromagnetic band gap structures," *Applied Computational Electromagnetics Society Journal*, vol. 33, no. 3, pp. 305-311, 2018.
- [12] J. Jiang, Y. Li, L. Zhao, and X. Liu, "Wideband MIMO directional antenna array with a simple metamaterial decoupling structure for X-band applications," *Applied Computational Electromagnetics Society Journal*, vol. 35, no. 5, pp. 556-566, 2020.
- [13] I. Adam, M. N. M. Yasin, N. Ramli, M. Jusoh, H. A. Rahim, T. B. A. Latef, T. F. T. M. N. Izam, and T. Sabapathy, "Mutual coupling reduction of a wideband circularly polarized microstrip MIMO antenna," *IEEE Access*, vol. 7, pp. 97838-97845, July 2019.
- [14] J. Iqbal, U. Illahi, M. I. Sulaiman, M. M. Alam, M. M. SU'UD, and M. N. M. Yasin, "Mutual coupling reduction using hybrid technique in wideband circularly polarized MIMO antenna for WiMAX application," *IEEE Access*, vol. 7, pp. 40951-40958, Apr. 2019.
- [15] N. Hussain, M.-J. Jeong, J. Park, and N. Kim, "A broadband circularly polarized Fabry-Perot resonant antenna using a single-layered PRS for 5G MIMO application," *IEEE Access*, vol. 7, pp. 40897-42907, Apr. 2019.
- [16] M. Y. Jamal, M. Li, and K. L. Yeung, "Isolation enhancement of closely packed dual circularly polarized MIMO antenna using hybrid technique," *IEEE Access*, vol. 8, pp. 11241-11247, Jan. 2020.
- [17] K. L. Chung, A. Cui, and B. Feng, "A Guo-shaped patch antenna for hidden WLAN access points," *Int. J. RF & Microw. Comp. Aided Eng.*, mmce.22323, July 2, 2020.
- [18] CST Microwave Studio, ver. 2017, Computer Simulation Technology, Framingham, MA, 2017.
- [19] K. L. Chung, "A wideband circularly polarized H-shaped patch antenna," *IEEE Trans. Antennas Propag.*, vol. 58, no. 7, pp. 3379-3383, July 2010.
- [20] K. L. Chung, W. Li, Y. Li, R. Liu, and P. Zhang, "Chinese character-shaped artistic patch antenna," *IEEE Antennas Wireless Propag. Lett.*, vol. 18, no. 8, pp. 1542-1546, Aug. 2019.
- [21] S. Blanch, J. Romeu, and I. Corbella, "Exact representation of antenna system diversity performance from input parameter description," *Electron. Lett.*, vol. 39, no. 9, p. 705, 2003.



Kwok L. Chung (Senior Member, IEEE) is a Research Professor and a Supervisor of Ph.D. students with Qingdao University of Technology (QUT). He is also a Director of Civionics Research Laboratory where he leads a cross-disciplinary research team at QUT. His current research interests include passive wireless sensors, cement-based materials design and characterization, microwave antennas, and metasurface. He is the Founding Chair of the IEEE Qingdao AP/MTT/COM joint chapter (CN10879) under Beijing Section. He has been an Associate Editor of IEEE ACCESS and an Associate Editor of Elsevier Alexandria Engineering Journal since 2016 and 2020, respectively. He serves as a Reviewer for the numerous IEEE, IET, Elsevier, and other international journals.



Aiqi Cui was born in Jincheng, Shanxi, China in 1994. She received a degree in Packaging Engineering from Hunan University of Technology. She is currently pursuing a master's degree in Material Science and Engineering. Her research interests include electromagnetic shielding, material characterization, and artistic antennas.

Mingliang Ma received the B.S. degree from Ludong University in 2007, and received Ph.D. degree in Materials Science from North-western Polytechnical University in 2014. In late 2014, he joined the Qingdao University of Technology and now is an Associate Professor. His main research areas include design of multi-functional electromagnetic absorption materials, and disaster prevention mitigation and protection engineering.



Botao Feng (Senior Member, IEEE) received the Ph.D. degree in Communication and Information System from the Beijing University of Posts and Telecommunications (BUPT), Beijing, China, in 2015. He is currently a Postgraduate Advisor and a Postdoctoral Advisor with Shenzhen University, China, where he is also the Head of the Laboratory of Wireless Communication, Antennas and Propagation and the Deputy Director of the Department of Electronic Science and Technology.